(11) Kranig, W.; Hüser, B.; Spiess, H. W.; Kreuder, W.; Ringsdorf, H.; Zimmermann, H. *Adv. Mater.* **1990**, *2*, 36.
(12) Ringsdorf, H.; Wüstefeld, R.; Zerta, E.; Ebert, M.; Wendorff, J. H. *Angew. Chem.* **1989**, *101*, 934.
(13) Spiess, H. W. In *Advances in Polymer Science*; Kausch, H. H., Zachmann, H. G., Eds.; Springer-Verlag: Berlin, 1985; Vol. 66.
(14) Müller, K.; Meier, P.; Kothe, G. *Prog. NMR Spectrosc.* **1985**, *17*, 211.
(15) Goldfarb, D.; Luz, Z.; Zimmermann, H.; *Isr. J. Chem.* **1983**, *23*, 341.
(16) Kranig, W.; Spiess, H. W.; Karthaus, O.; Wüstefeld, R.; Ringsdorf, H. *Liq. Cryst.*, in press.
(17) Kranig, W. Diploma Thesis, Universität Mainz, 1987.
(18) Hüser, B. Ph.D. Thesis, Universität Mainz, 1988.
(19) Vallerien, S. U.; Kremer, F.; Hüser, B.; Spiess, H. W. *Colloid Polym. Sci.* **1989**, *267*, 583.
(20) Hsu, T. C.; Hüser, B.; Pakula, T.; Spiess, H. W.; Stamm, M. *Makromol. Chem.*, in press.
(21) Ebelhäuser, R. Ph.D. Thesis, Universität Mainz, 1985.
(22) Lifshitz, E.; Goldfarb, D.; Vega, S.; Luz, A.; Zimmermann, H. *J. Am. Chem. Soc.* **1987**, *109*, 7280.
(23) Westermark, B.; Spiess, H. W. *Makromol. Chem.* **1988**, *189*, 2367.

Registry No. 1, 128270-08-6; 2, 128302-21-6; 3, 128302-22-7; 4 (dimer), 128302-23-8.

Mean-Square Radius of Gyration of Oligo- and Poly(methyl methacrylate)s in Dilute Solutions

Yoshinori Tamai, Toshiki Konishi, Yoshiyuki Einaga, Motoharu Fujii,† and Hiromi Yamakawa*

Department of Polymer Chemistry, Kyoto University, Kyoto 606, Japan

Received January 17, 1990

ABSTRACT: The mean-square radius of gyration $\langle S^2 \rangle$ was determined by small-angle X-ray scattering and light scattering for 20 samples of atactic oligo- and poly(methyl methacrylate)s (a-PMMA), each with the fraction of racemic diads $f_r = 0.79$, in the range of weight-average molecular weight M_w from 4.02×10^2 to 2.83×10^6 in acetonitrile at 44.0 °C (Θ). The ratio $\langle S^2 \rangle / x_w$ as a function of the weight-average degree of polymerization, x_w, exhibits unusual behavior; it passes through a maximum at $x_w \simeq 50$ before reaching its asymptotic value for large x_w. First, a comparison is made of the experimental data with the theoretical values on the basis of three types of the rotational isomeric state model, and it is shown that none of them can explain the observed maximum. Then, it is shown that the helical wormlike (HW) chain theory may well explain the data with the parameter values $\lambda^{-1}\kappa_0 = 4.0$, $\lambda^{-1}\tau_0 = 1.1$, $\lambda^{-1} = 57.9$ Å, and $M_L = 36.3$ Å^{-1}, where κ_0 and τ_0 are the curvature and torsion, respectively, of the characteristic helix taken at the minimum of energy, λ^{-1} is the stiffness parameter, and M_L is the shift factor. The present a-PMMA chain has a larger λ^{-1} (stiffness) but smaller Kuhn segment length (average chain dimension for large x_w) than an atactic polystyrene chain ($f_r = 0.59$), on which a similar study was previously made. In order to illustrate the situation, a picture is given of representative instantaneous contours of HW Monte Carlo chains for the two polymers.

Introduction

In this series of experimental work on dilute solutions of oligomers and polymers, we have already determined the mean-square optical anisotropy $\langle \Gamma^2 \rangle$, intrinsic viscosity $[\eta]$, and mean-square radius of gyration $\langle S^2 \rangle$ for atactic polystyrene (a-PS), using well-characterized samples of narrow molecular weight distribution and fixed stereochemical composition (the fraction of racemic diads $f_r = 0.59$),[1-4] and analyzed the data at the Θ temperature on the basis of the helical wormlike (HW) chain model.[5-9] As a next step, in the present and forthcoming papers, we proceed to make a study on atactic poly(methyl methacrylate) (a-PMMA) in the same spirit, using well-characterized samples over a wide range of molecular weight M, including the oligomer region, and with $f_r = 0.79 \pm 0.01$.[10] The present paper deals with only $\langle S^2 \rangle$.

Now, there have already been a number of both experimental and theoretical investigations[11-19] on dilute solutions of a-PMMA or syndiotactic poly(methyl methacrylate) (s-PMMA). Among these, the most remarkable experiment is due to Kirste and Wunderlich,[14,15] who showed that the so-called Kratky plot of the scattering function, $P(\theta)$, determined from small-angle X-ray scattering (SAXS) exhibits damped oscillation around an asymptotic straight line for the rodlike polymer. On the theoretical side, Yoon and Flory[19] showed on the basis of the rotational isomeric state (RIS) model that, for PMMA chains with an f_r greater than a certain value, the characteristic ratio C_n first increases with increasing chain length, then passes through a maximum, and finally goes down to its asymptotic value C_∞. These results are inconsistent with the theoretical predictions based on the Gaussian chain and even on the Kratky–Porod (KP) wormlike chain,[20] and indeed this led us to the introduction of the HW chain model.[5-7]

We have already made an analysis of some of the literature data for $[\eta]$ and $\langle S^2 \rangle$ as functions of M for a- (or s-)PMMA on the basis of the HW model[9,21] and preliminarily concluded, from a comparison with the results for the a-PS,[2-4] that there is a remarkable difference between chain conformations of these two polymers.[3,4] However, the existent data for a-PMMA scatter considerably and are not good enough to permit an accurate determination of the HW model parameters for a quantitative discussion of its chain conformations in dilute

† Present address: Research Laboratory, Dic-Hercules Chemicals, Inc., Yahatakaigan-dori, Ichihara, Chiba 290, Japan.

0024-9297/90/2223-4067$02.50/0

solution. This is the reason why we have undertaken its precise experimental study.

The HW model parameters to be determined are the curvature, κ_0, and torsion, τ_0, of the characteristic regular helix taken at the minimum of energy, the stiffness parameter, λ^{-1}, as defined as the bending force constant divided by $k_BT/2$ with k_B the Boltzmann constant and T the absolute temperature, and the shift factor, M_L, as defined as the molecular weight per unit contour length. In anticipation of the results, we note that these four parameters for the a-PMMA may be rather accurately determined from an analysis of the present data only for $\langle S^2 \rangle$ (at Θ), since the ratio $\langle S^2 \rangle / M$ as a function of M exhibits a maximum. Recall that such a determination is impossible in the case of the a-PS, for which $\langle S^2 \rangle / M$ increases monotonically with increasing M to its asymptotic value. In order to illustrate the difference between the two polymers, we also give a picture of representative instantaneous contours of HW Monte Carlo chains generated with the model parameters determined for them.

The present data for $\langle S^2 \rangle$ are also compared with the theoretical values calculated on the basis of the RIS models of Flory et al.[22,23] and of Sundararajan,[24] for comparison.

Experimental Section

Materials. The a-PMMA samples, including the oligomers, used in this work were prepared by group-transfer polymerization (GTP)[10,25,26] for the weight-average molecular weight $M_w \lesssim 2 \times 10^5$ and by radical polymerization for $M_w \gtrsim 2 \times 10^5$. The GTP was carried out in tetrahydrofuran at 0 °C with tris(dimethylamino)sulfonium (trimethylsilyl)difluoride ($(Me_2N)_3S^+SiMe_3F_2^-$) as a coinitiator, and the radical polymerization, in bulk at 60 °C with azobis(isobutyronitrile) as an initiator. Both of the two terminal groups of the samples prepared by the GTP are hydrogen atoms. In the radical polymerization, the reaction was terminated at such a low yield as 8 or 10% in order to suppress possible chain branching.

The original samples synthesized were separated into fractions of narrow molecular weight distribution by preparative gel permeation chromatography (GPC) with two serially connected Tosoh G2000H_6 (600 × 50 mm) columns using chloroform as an eluent at a flow rate of 18 mL/min for the samples with $M_w <$ 5000 and by fractional precipitation using benzene as a solvent and methanol as a precipitant for the other samples. The fraction designated OM51 was obtained by fractional precipitation, followed by further separation by GPC with four serially connected Tosoh GMH_{XL} columns using chloroform as an eluent. The fractionation by GPC and fractional precipitation were repeated several times.

The samples with $M_w < 1000$ were dissolved in chloroform or benzene, filtered through an ultracellafilter membrane of pore size 0.22 μm, and then dried under vacuum at 40–80 °C for 3–14 days. The samples with $M_w > 1000$ were freeze-dried from their benzene solutions after filtration through the membrane.

Solvents used for light-scattering (LS) and SAXS measurements were purified according to standard procedures. Solvents used for NMR spectroscopy were of reagent grade.

^{1}H and ^{13}C NMR. ^{1}H and ^{13}C NMR spectra of the samples Mr8 and Mr28 prepared by radical polymerization were recorded on a JEOL JNM GX-400 spectrometer in chloroform-*d* containing tetramethylsilane as an internal standard at 55 °C. The polymer concentrations were 2.3 wt % for Mr8 and 1.8 wt % for Mr28. The instrument was operated with frequencies of 399.8 MHz for ^{1}H NMR and 100.5 MHz for ^{13}C NMR. Measurements of the NMR spectra were made by using a radio frequency pulse angle of 90° with pulse repetition times of 34.1 s for ^{1}H NMR and 10.8 s for ^{13}C NMR, which are more than 5 times as long as the longest spin–lattice relaxation times of the respective nuclides. In the ^{13}C NMR experiments, the nuclear Overhauser effect was eliminated by the gated decoupling method.

Light Scattering. LS measurements were carried out to determine the weight-average molecular weights M_w of the samples with $M_w > 1.0 \times 10^3$, the Θ temperature of acetonitrile solutions, and $\langle S^2 \rangle$ for the samples with $M_w > 2 \times 10^5$ in acetonitrile at Θ. In the determination of M_w, we used two different solvents, depending on M_w: acetone at 25.0 °C for M_w ranging from 10^3 to 10^4 and acetonitrile at Θ for $M_w > 10^4$. For the determination of Θ, the second virial coefficient, A_2, was measured for several samples at several temperatures ranging from 30 to 60 °C.

A Fica 50 light-scattering photometer was used for all the measurements with an incident light of wavelength 436 nm. For calibration of the apparatus, the intensity of light scattered from pure benzene was measured at 25.0 °C at a scattering angle 90° with the incident light of wavelength 436 nm, where the Rayleigh ratio of pure benzene at 25 °C was taken as 46.5×10^{-6} cm^{-1}. The depolarization ratio ρ_u of pure benzene at 25.0 °C was determined to be 0.41 ± 0.01 by the method of Rubingh and Yu.[27a] Although vertically polarized incident light was used in most cases, measurements with unpolarized incident light were also carried out for acetone solutions to make corrections for the optical anisotropy. Scattering intensities were measured for the solutions of five different concentrations and at scattering angles ranging from 30 to 150°. The obtained data were analyzed by an application of the Berry square-root plot.[27b]

In anticipation of the results, we note that the Θ temperature of acetonitrile solutions of a-PMMA is 44.0 °C, while acetone is a good solvent for it. Thus, the most concentrated solutions of each sample in acetone and acetonirile were prepared by continuous stirring for 1 day at room temperature and ca. 50 °C, respectively. These solutions and the solvents were optically purified by filtration through an ultracellafilter membrane of pore size 0.45 or 0.1 μm. The solutions of lower concentrations were obtained by successive dilution. The weight concentrations of test solutions were determined gravimetrically and converted to mass concentrations, c, by using the densities of the solutions.

The refractive index increment, $\partial n/\partial c$, was measured at 436 nm for a-PMMA samples with low to high molecular weights in acetone at 25.0 °C and for samples with high molecular weights in acetonitrile at 44.0 °C (Θ) by the use of a Shimadzu differential refractometer. For the acetone solutions, $\partial n/\partial c$ increased from 0.120 to 0.133_5 cm^3/g as M_w was increased from 1100 to 5060, and it remained constant for higher M_w. The value in acetonitrile was 0.144 cm^3/g for $M_w > 10^4$.

Small-Angle X-ray Scattering. SAXS measurements were carried out for acetonitrile solutions of the a-PMMA samples with $M_w < 2 \times 10^5$ at 44.0 °C (Θ) by using an Anton Paar Kratky U-slit camera with an incident X-ray of wavelength 1.54 Å (Cu Kα line). The apparatus system and the methods of data acquisition and analysis are the same as those described in a previous paper.[4]

The measurements were performed for five solutions of different concentrations for each polymer sample and for the solvent at angles ranging from 1×10^{-3} rad to a value at which the intensity became negligibly small. Here, collimation of the incident beam was carefully achieved to minimize the intensity of parasitic scattering and the tail of the transmitted X-ray. Corrections for the stability of the X-ray source and the detector electronics were made by measuring the intensity scattered from Lupolene (a platelet of polyethylene) used as a working standard before and after each measurement for a given sample solution. The effect of the absorption of X-ray by a given solution or solvent was also corrected by measuring the scattering intensity from Lupolene with insertion of the solution or solvent in between the X-ray source and Lupolene. The excess reduced intensities, $\Delta I_R(\theta)$, at scattering angle θ were obtained from the observed (smeared) excess-reduced intensities by the desmearing procedure, which consists of expressing the true scattering function in terms of cubic B-spline functions, as described before.[4] All the data were processed by the use of a FACOM M780 digital computer in this university.

The desmeared excess-reduced intensities, $\Delta I_R(\theta)$, for solutions of polymer mass concentration c were analyzed by the square-root plot based on

$$[Kc/\Delta I_R(\theta)]^{1/2} = [1/M_w P(k)]^{1/2} + \mathcal{O}(c) \quad (1)$$

with

$$K = \varphi_A'^2 \Delta z_e^2 \quad (2)$$

In eq 1, $P(k)$ is the scattering function and may be expanded as

Table I
Values of M_w, x_w, and M_w/M_n for Atactic Oligo- and Poly(methyl methacrylate)s

sample	M_w	x_w	M_w/M_n
OM4	4.02×10^2	4	1.00
OM5	5.02×10^2	5	1.00
OM6	6.02×10^2	6.00	1.00
OM7	7.09×10^2	7.07	1.00
OM8	7.98×10^2	7.96	1.00
OM11[a]	1.10×10^3	11.0	1.04
OM18	1.80×10^3	18.0	1.07
OM22	2.23×10^3	22.3	1.06
OM30	2.95×10^3	29.5	1.06
OM51	5.06×10^3	50.6	1.08
MM1[b]	1.09×10^4	109	1.06
MM2	1.90×10^4 (1.88×10^4)	190	1.08
MM4	3.53×10^4	353	1.07
MM5	5.16×10^4 (5.04×10^4)	516	1.07
MM7	7.40×10^4	740	1.09
MM12	1.19×10^5 (1.18×10^5)	1190	1.09
Mr4	3.61×10^5 (3.56×10^5)	3610	1.07
Mr8	7.58×10^5 (7.62×10^5)	7580	1.05
Mr19	1.90×10^6	19000	1.06
Mr28	2.83×10^6	28300	1.10

[a] M_w's of OM11 through OM51 were determined in acetone. [b] M_w's of MM1 through Mr28 were determined in acetonitrile, the figures in parentheses representing the values in acetone.

$$P(k) = 1 - (1/3)\langle S^2\rangle_s k^2 + \mathcal{O}(k^4) \quad (3)$$

where $\langle S^2\rangle_s$ is the apparent mean-square radius of gyration and k is the magnitude of the scattering vector

$$k = (4\pi/\lambda_0) \sin(\theta/2) \quad (4)$$

with λ_0 the wavelength of the incident X-ray. Note that eq 3 is rather the defining equation for $\langle S^2\rangle_s$. In eq 2, φ_A' is the apparatus constant, and Δz_e is the mole number of effective electrons per gram of the solute polymer and is given by

$$\Delta z_e = (n_2/M_0) - (v_2\rho_0 n_1/M_s) \quad (5)$$

where n_2 and M_0 are the number of electrons and the molecular weight per repeat unit of the polymer, respectively, v_2 is the partial specific volume of the polymer, ρ_0 is the density of the solvent, and n_1 and M_s are the number of electrons and the molecular weight of the solvent molecule, respectively. The value 0.7557 g/cm^3 was used for ρ_0 of acetonitrile at 44.0 °C, and the values of v_2 were determined from density measurements in this solvent at 44.0 °C.

The test solutions were prepared gravimetrically and made homogeneous by continuous stirring for 1–5 days at ca. 50 °C.

Results

Molecular Weights and Their Distributions. The values of M_w, the weight-average degree of polymerization, x_w, and the ratio of M_w to the number-average molecular weight, M_n, determined for the a-PMMA samples we used for the measurements of $\langle S^2\rangle$ are given in Table I. Note that the samples OM3 and MM12′, which were used only for the determination of f_r, and also the sample MM19′, which was used only for the determination of Θ, are omitted in the table. From analytical GPC measurements, the oligomer samples OM3, OM4, and OM5 were found to be completely monodisperse. The samples OM3 and OM4 were confirmed by mass and ^{1}H NMR spectroscopy to be the trimer and tetramer, respectively, and the sample OM5 was confirmed by analytical GPC to be the pentamer. The other oligomer samples OM6, OM7, and OM8 were also identified from the analytical GPC. However, it was then found that each of them contained a certain amount of the neighboring homologues; OM6 contained 2.8 wt % of the pentamer and 2.8 wt % of the heptamer, OM7 contained 2.8 wt % of the hexamer and 9.7 wt % of the octamer, and OM8 contained 11.6 wt % of the heptamer and 7.8 wt % of the nonamer. For these oligomer samples, the values of M_w and M_n were calculated from their molecular weight distributions thus determined.

Table II
Values of f_r Determined from ^{1}H and ^{13}C NMR Spectra

sample	f_r	sample	f_r
OM3	0.80[a]	MM12′	0.79[a]
OM4	0.78[a]	Mr8	0.79
OM5	0.78[a]	Mr28	0.79
MM5	0.78[a]		

[a] See ref 10.

For the other samples with $M_w > 1.0 \times 10^3$, the values of M_w were directly determined from the LS measurements, and those of M_w/M_n, from the analytical GPC. The figures in parentheses in Table I represent the values of M_w determined in acetone, which are in good agreement with those in acetonitrile. This indicates that the possible molecular association in acetonitrile[28] does not occur at least in dilute solution at 44 °C. The results for M_w/M_n from the GPC analysis confirm that the molecular weight distributions of all the test samples are sufficiently narrow for the present purpose.

Stereochemical Compositions. The fractions of racemic diads, f_r, of the samples OM3, OM4, OM5, MM5, and MM12′, which were prepared by GTP, had already been determined from their ^{1}H and ^{13}C NMR spectra in a previous paper.[10] Thus, in the present study, we determined f_r of the high molecular weight samples Mr8 and Mr28 prepared by radical polymerization in order to confirm that the samples prepared by the two different methods have the same value of f_r. The determination of f_r was accomplished by analyzing the intensity distributions of the ^{1}H and ^{13}C NMR peaks, which were assigned to the specific proton or carbon atoms with the aid of the peak assignment given by Chûjô et al.,[29] assuming that the distribution of the racemic and meso diads in the a-PMMA chain is Bernoullian. The validity of this assumption was justified by the good agreement between the calculated and observed distributions of the peak intensity, as in the case of the samples prepared by GTP.[10]

In Table II are given the values of f_r thus determined together with those obtained previously.[10] It is seen that the values of f_r are nearly equal to 0.79, almost independent of M_w and also of the method of polymerization. It is also concluded that the stereochemical sequences in the chains of all our a-PMMA samples obey Bernoullian statistics. This indicates that the RIS chains corresponding to our a-PMMA samples may be generated as random sequences of racemic and meso diads.

Θ Temperature. A_2 values multiplied by M_w are plotted against temperature for acetonitrile solutions in Figure 1. It is seen that A_2 vanishes at the same temperature independent of M_w provided that $M_w \gtrsim 5 \times 10^4$. Thus, this leads to the conclusion that the Θ temperature is 44.0 °C for acetonitrile solutions of a-PMMA with $f_r = 0.79$. (We confirmed that A_2 in fact vanishes in acetonitrile at 44.0 °C also for all the other samples for which we carried out the LS measurements of $\langle S^2\rangle$.) This value of Θ is very close to the value 45 °C reported by Fox.[13]

Mean-Square Radii of Gyration $\langle S^2\rangle_s$ and $\langle S^2\rangle$. The values of $(Kc/\Delta I_R)_{k=0}^{1/2}$ and $(Kc/\Delta I_R)_{c=0}^{1/2}$ for all the samples with $M_w \lesssim 1.2 \times 10^5$ listed in Table I in acetonitrile at Θ were evaluated from the square-root plots of the SAXS data for $Kc/\Delta I_R$ at finite scattering angles and concentrations with extrapolation to zero angle and concentration, respectively. They are plotted against c and

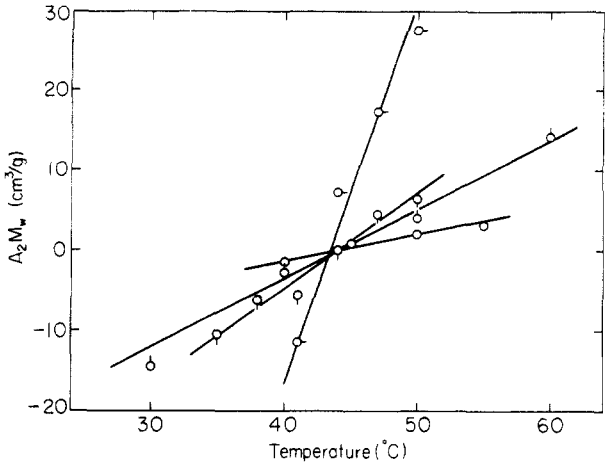

Figure 1. Plots of A_2M_w against temperature for the a-PMMA samples in acetonitrile: ○, MM5; ◌, MM19′ (M_w = 1.91 × 10⁵); ◔, Mr4; ○–, Mr19.

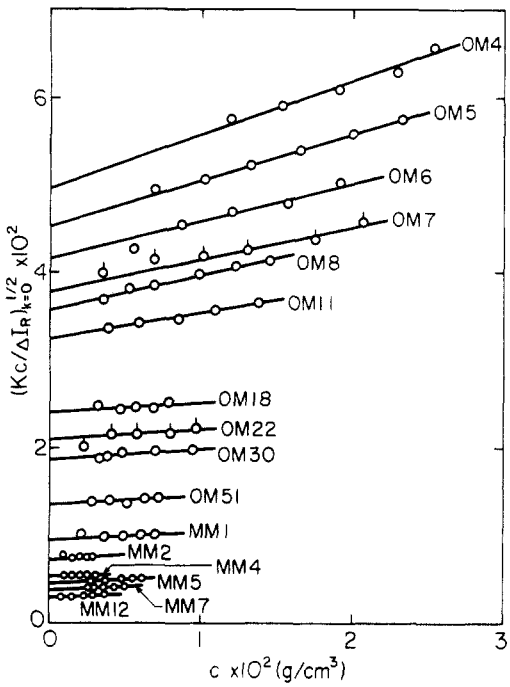

Figure 2. Plots of $(Kc/\Delta I_R)_{k=0}^{1/2}$ against c for the a-PMMA samples indicated in acetonitrile at 44.0 °C.

k^2 in Figures 2 and 3, respectively. Here the optical constant K was determined from eq 2 with the apparatus constant $\varphi_A' = 0.26_6$ cm³/mol determined previously[4] and with the values of Δz_e calculated with the value of v_2 for each sample with $M_w < 1.1 \times 10^4$ and with $v_2 = 0.820$ cm³/g for larger M_w.

In Figure 2, the straight line fitted to the data points for each sample with $M_w \lesssim 1.9 \times 10^4$ has a finite slope, indicating that A_2 does not vanish for the a-PMMA oligomers even in the Θ state. This is the same behavior as observed for the a-PS oligomers in cyclohexane at Θ.[4,30] However, we cannot argue the absolute values of A_2 themselves because of the large experimental uncertainty. In Figure 3, the data points for each sample also follow the indicated straight line, and $\langle S^2\rangle_s$ was evaluated from its slope. The values of $\langle S^2\rangle_s$ thus determined are listed in the second column of Table III. The common ordinate intercept for each sample in Figures 2 and 3 allows us to determine the value of M_w as given in the fourth column in Table III. (We could not determine M_w of the sample MM12 since we used another sample cell with φ_A' undetermined.) The values of M_w from the SAXS

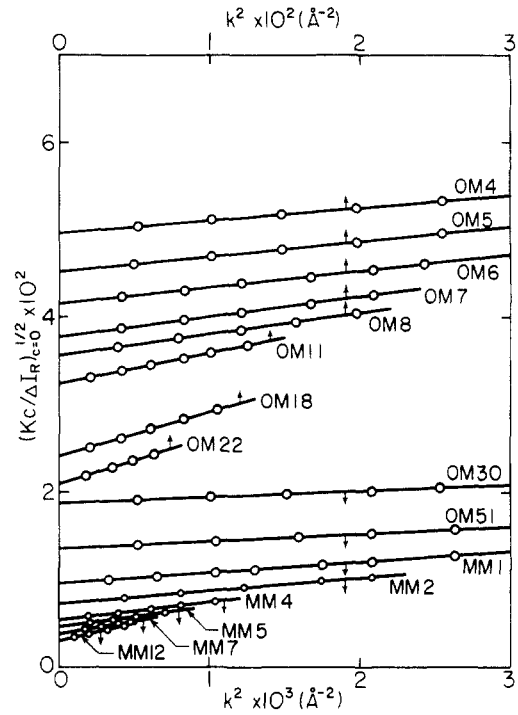

Figure 3. Plots of $(Kc/\Delta I_R)_{c=0}^{1/2}$ against k^2 for the a-PMMA samples indicated in acetonitrile at 44.0 °C.

Table III
Results of SAXS Measurements on Atactic Oligo- and Poly(methyl methacrylate)s in Acetonitrile at 44.0 °C

sample	$\langle S^2\rangle_s^{1/2}$, Å	$\langle S^2\rangle^{1/2}$, Å	M_w
OM4	4.1_5	2.9_7	$4.0_6 \times 10^2$
OM5	4.7_4	3.7_5	$4.8_9 \times 10^2$
OM6	5.1_8	4.3_0	$5.8_2 \times 10^2$
OM7	6.1_4	5.4_1	$7.0_2 \times 10^2$
OM8	6.5_1	5.8_3	$7.9_5 \times 10^2$
OM11	8.0_3	7.4_9	$9.5_0 \times 10^2$
OM18	$11._2$	$10._9$	$1.7_3 \times 10^3$
OM22	$12._6$	$12._3$	$2.3_1 \times 10^3$
OM30	$14._4$	$14._1$	$2.8_3 \times 10^3$
OM51	$19._1$	$18._9$	$5.4_6 \times 10^3$
MM1	$27._8$	$27._6$	$1.1_0 \times 10^4$
MM2	$35._5$	$35._4$	$1.9_3 \times 10^4$
MM4	$48._1$	$48._0$	$3.5_3 \times 10^4$
MM5	$56._5$	$56._4$	$4.9_6 \times 10^4$
MM7	$68._9$	$68._9$	$7.1_2 \times 10^4$
MM12	$87._6$	$87._5$	

measurements are seen to be rather in good agreement with those in Table I obtained by LS and other methods. The agreement demonstrates the accuracy of our SAXS measurements.

The values of $\langle S^2\rangle_s$ determined above contain contributions from the finite cross section of the polymer chain. Thus a correction must be made in order to draw from $\langle S^2\rangle_s$ the mean-square radius of gyration $\langle S^2\rangle$ of the chain contour, since the theoretical values to be compared are given for the latter. For a continuous chain having a uniform circular cross section of diameter d, $\langle S^2\rangle_s$ may be expressed as

$$\langle S^2\rangle_s = \langle S^2\rangle + S_c^2 \tag{6}$$

with S_c the radius of gyration of the cross section, i.e., $S_c^2 = d^2/8$, as shown previously.[4] The diameter d may be calculated from the relation $d = 2(v_2M_L/\pi N_A)^{1/2}$. In this work, we have obtained 8.2 Å for d with the value 0.82 cm³/g for v_2 determined for the a-PMMA sample of sufficiently large M_w in acetonitrile at Θ and with the value 38.6 Å⁻¹ for M_L corresponding to the a-PMMA chain fully extended to the all-trans conformation.[31] As is seen from

Table IV
Results of LS Measurements on Atactic Poly(methyl methacrylate) in Acetonitrile at 44.0 °C

sample	$10^{-6}M_w$	$10^{-2}\langle S^2\rangle^{1/2}$, Å
Mr4	0.361	1.5_6
Mr8	0.758	2.2_4
Mr19	1.90	3.5_4
Mr28	2.83	4.3_5

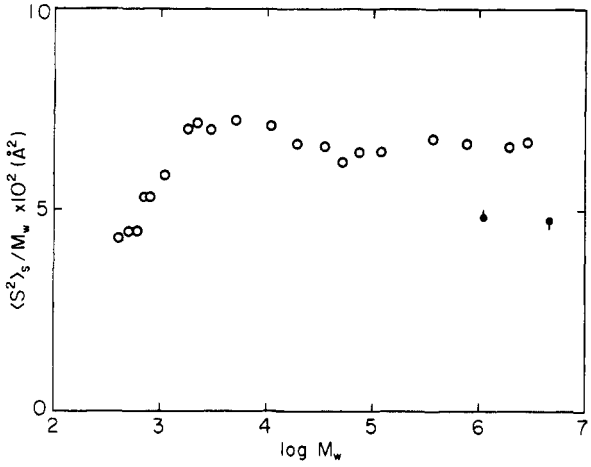

Figure 4. Molecular weight dependence of $\langle S^2\rangle_s/M_w$ for a-PMMA: ○, present data in acetonitrile at 44.0 °C; ♦ and ♦, LS data in *n*-butyl chloride at 35.4 and 32.6 °C, respectively, by Schulz and Kirste.[11]

Table III, the contribution of S_c^2 to $\langle S^2\rangle_s$ amounts to about 50% for the tetramer, but progressively diminishes with increasing molecular weight, and becomes negligible for $M_w > 2 \times 10^4$.

Table IV summarizes the results for $\langle S^2\rangle$ for the samples with $M_w \gtrsim 3.6 \times 10^5$ from LS measurements in acetonitrile at 44.0 °C (Θ) together with those for M_w.

Molecular Weight Dependence of $\langle S^2\rangle_s/M_w$. Figure 4 shows a plot of the ratio $\langle S^2\rangle_s/M_w$ against the logarithm of M_w (of Table I) for the present results (unfilled circles) for a-PMMA in acetonitrile at 44.0 °C (Θ) by SAXS and LS. The SAXS data are smoothly connected to the LS data, the latter being almost independent of M_w. As M_w is increased, the ratio $\langle S^2\rangle_s/M_w$ increases for $M_w < 10^3$, then passes through a maximum, and finally approaches its asymptotic value for $M_w > 10^5$.

The filled circles with pip up and pip down in Figure 4 represent the LS results of Schulz and Kirste[11] for a-PMMA with $f_r = 0.8$ in *n*-butyl chloride at 35.4 and 32.6 °C (Θ), respectively. Their data are significantly lower than ours in acetonitrile at Θ. The discrepancy is too large to be attributed to the solvent effect and may possibly be due to the fact that they determined $\langle S^2\rangle$ at considerably low temperatures (Θ). (We note that our Θ temperature determined preliminarily for a-PMMA with $f_r = 0.79$ in *n*-butyl chloride is 40.8 °C and also that this solvent cannot be used for SAXS measurements because of the strong absorption of X-rays.)

Discussion

Comparison with RIS Values. Figure 5 shows a plot of the ratio $\langle S^2\rangle/x_w$ against the logarithm of x_w for the a-PMMA in acetonitrile at 44.0 °C (Θ). The most remarkable feature is that $\langle S^2\rangle/x_w$ passes through a maximum at $x_w \simeq 50$ before reaching its asymptotic value at higher x_w. We believe that this dependence of $\langle S^2\rangle/x_w$ on x_w arises from the fact that the a-PMMA chain may possibly take locally a helical conformation in dilute solution. It is evident that the present finding cannot be explained by the KP wormlike chain model.[20]

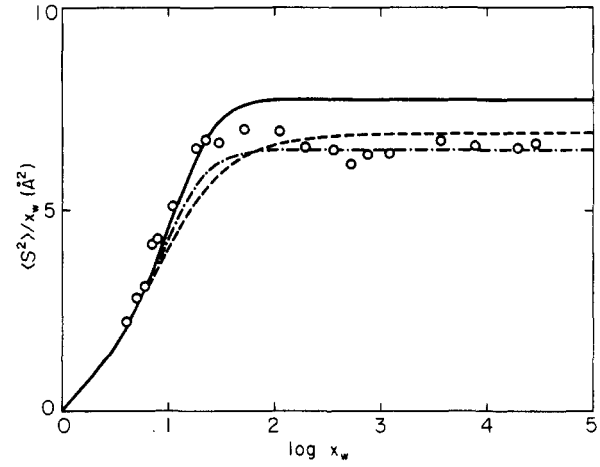

Figure 5. Plots of $\langle S^2\rangle/x_w$ against log x_w for a-PMMA with $f_r = 0.79$: ○, present data in acetonitrile at 44.0 °C. The solid, dashed, and dot-dashed curves represent the corresponding RIS values with the parameters of Sundararajan and Flory,[22] Vacatello and Flory,[23] and Sundararajan,[24] respectively.

Now, we make a comparison of the experimental results for $\langle S^2\rangle$ with the theoretical values on the basis of the three RIS models, i.e., the 2-state model by Sundararajan and Flory,[22] the 6-state model by Vacatello and Flory,[23] and the 3-state model by Sundararajan.[24] As in a previous RIS calculation of $\langle S^2\rangle$ for the a-PS chain,[4] we have calculated $\langle S^2\rangle$ for the α-carbon atoms of a-PMMA following the matrix algebra developed by Flory[32,33] with the use of the modified generator matrix given by eq C2 of ref 4. The RIS chains for the a-PMMA with $f_r = 0.79$ have been generated by the Monte Carlo method, considering the fact that the racemic and meso diads are randomly distributed in the chains of our samples. In the 3-state model, the energy parameters in the statistical weight matrices have been adjusted so that the calculated asymptotic value of $\langle S^2\rangle/x$ (with x the degree of polymerization) agrees with the observed one, since only the allowable range of each parameter is given by Sundararajan.[24] For the other parameters in the 3-state model and the parameters in the other two models, the values given in the original papers have been adopted. In the evaluation of $\langle S^2\rangle$, the effect of chain ends cannot be neglected for short chains. Thus, the fact that both terminal groups of our a-PMMA chains prepared by GTP are hydrogen atoms has been taken into account by modifying the statistical weight matrices only near the terminal ends as described in Appendix A. The matrices for the internal bonds have been unchanged from those given in the original papers.

The RIS theoretical values of $\langle S^2\rangle/x$ thus calculated are also shown in Figure 5. Those for the three models are in good agreement with each other and also with the experimental data for $x_w \leq 6$. This indicates that the present correction of the finite cross section for $\langle S^2\rangle_s$ is rather reasonable, as in the case of a-PS analyzed in a previous paper.[4] However, none of these models can predict the occurrence of the maximum found experimentally. The 2-state and 6-state models give asymptotic values appreciably larger than the experimental value. These discrepancies may also require reconsideration of the rotational isomeric states and/or the energy parameters in the statistical weight matrices proposed for PMMA by the above authors.

Values of the HW Model Parameters. Figure 6 shows a comparison of the present results (unfilled circles) for $\langle S^2\rangle/x_w$ as a function of x_w with the previous ones (filled

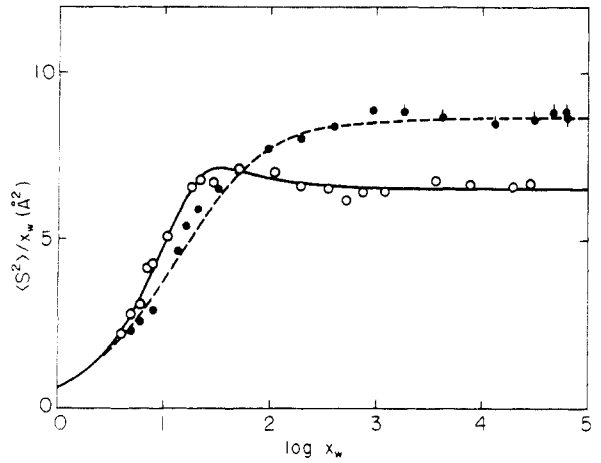

Figure 6. Plots of $\langle S^2\rangle/x_w$ against log x_w for the a-PMMA samples with $f_r = 0.79$ in acetonitrile at 44.0 °C and for a-PS with $f_r = 0.59$ in cyclohexane at 34.5 °C: ○, present data for a-PMMA; ♀, SAXS data for a-PS by Konishi et al.;[4] ♦, LS data for a-PS by Miyaki;[34] ♦, LS data for a-PS by Miyaki et al.[35] The solid and dashed curves represent the best fit HW theoretical values calculated with the model parameters listed in Table V for a-PMMA and a-PS, respectively.

circles) for a-PS in cyclohexane at Θ,[4] including the data by Miyaki et al.[34,35] It is seen that there is a remarkable difference between them. For the a-PMMA, the ratio $\langle S^2\rangle/x_w$ first increases more rapidly with increasing x_w, then exhibits a maximum, as stated above, and finally goes down to its asymptotic value, while for the a-PS, it increases monotonically and reaches the asymptotic value higher by about 32% than the former. This difference between the two chains in the behavior of $\langle S^2\rangle$ may possibly be due to the difference in the local chain structure and stiffness. In the following, we discuss the result quantitatively on the basis of the HW model.[5-7]

For the HW chain of contour length L (without excluded volume), $\langle S^2\rangle$ is given by[6,7]

$$\langle S^2\rangle = \lambda^{-2} f(\lambda L; \lambda^{-1}\kappa_0, \lambda^{-1}\tau_0) \tag{7}$$

where the function f is defined by

$$f(L;\kappa_0,\tau_0) = \frac{\tau_0^2}{\nu^2} f_{KP}(L) + \frac{\kappa_0^2}{\nu^2}\left[\frac{L}{3r}\cos\varphi - \frac{1}{r^2}\cos(2\varphi) + \frac{2}{r^3 L}\cos(3\varphi) - \frac{2}{r^4 L^2}\cos(4\varphi) + \frac{2}{r^4 L^2}e^{-2L}\cos(\nu L + 4\varphi)\right] \tag{8}$$

with

$$\nu = (\kappa_0^2 + \tau_0^2)^{1/2} \tag{9}$$

$$r = (4 + \nu^2)^{1/2} \tag{10}$$

$$\varphi = \cos^{-1}(2/r) \tag{11}$$

and with f_{KP} being the function f for the KP chain given by

$$f_{KP}(L) = \frac{L}{6} - \frac{1}{4} + \frac{1}{4L} - \frac{1}{8L^2}(1 - e^{-2L}) \tag{12}$$

In the limit $\lambda L \to \infty$, we have

$$\lim_{\lambda L\to\infty} f(\lambda L)/\lambda L = \frac{1}{6}c_\infty \tag{13}$$

with

$$c_\infty = \frac{4 + (\lambda^{-1}\tau_0)^2}{4 + (\lambda^{-1}\kappa_0)^2 + (\lambda^{-1}\tau_0)^2} \tag{14}$$

Then, $\langle S^2\rangle/x$ and x are related to $f(\lambda L)$ and L as

$$\langle S^2\rangle/x = (M_0\lambda^{-1}/M_L)[f(\lambda L;\lambda^{-1}\kappa_0,\lambda^{-1}\tau_0)/\lambda L] \tag{15}$$

and

$$\log x = \log(\lambda L) + \log(\lambda^{-1}M_L/M_0) \tag{16}$$

respectively. (Recall that M_0 is the molecular weight of the repeat unit.) From eqs 13 and 15, the asymptotic value of $\langle S^2\rangle/x$ is seen to be equal to $M_0\lambda^{-1}c_\infty/6M_L$. The solid curve in Figure 6 represents the best fit HW theoretical values for a-PMMA. It is seen that they can reproduce quantitatively the behavior of $\langle S^2\rangle/x_w$ as a function of x_w over the whole range of x_w examined, as in the case of a-PS, for which the corresponding theoretical values are represented by the dashed curve.

The values of the HW model parameters thus determined by the curve fitting are summarized in Table V together with those for a-PS[4] obtained from $\langle\Gamma^2\rangle$ and $\langle S^2\rangle$. The value of M_L for a-PMMA is slightly smaller than the value 38.6 Å^{-1} corresponding to the chain fully extended to the all-trans conformation.[31] The a-PMMA and a-PS chains have the significantly different values of $\lambda^{-1}\tau_0$, while the values of $\lambda^{-1}\kappa_0$ are approximately the same, the value of $\lambda^{-1}\tau_0$ for a-PMMA being only one-tenth of that for a-PS. It then follows that the characteristic regular helices for the two polymer chains are very different in shape, as shown below. The values of λ^{-1} indicate that the helical form is locally preserved in dilute solution, to a greater extent, in the a-PMMA chain than in the a-PS chain, or in other words, the former chain is stiffer than the latter. This may be in conflict with the fact that the asymptotic value of $\langle S^2\rangle/x_w$ for large x_w, or the characteristic ratio C_∞, for a-PMMA is smaller than that for a-PS. The latter fact has often led to the conclusion, which is wrong in our opinion, that a-PS is a less flexible polymer than a-PMMA. It should be pointed out here that $(\langle S^2\rangle/x_w)_{x_w=\infty}$ or C_∞ depends not only on the stiffness but also on the local conformation of the polymer chain, as seen from eqs 13–15.

The point may be more clarified by the introduction of the Kuhn statistical segment length, A_K, defined by

$$A_K = \lim_{L\to\infty}\langle R^2\rangle/L = 6M_L\lim_{M\to\infty}\langle S^2\rangle/M \tag{17}$$

where $\langle R^2\rangle$ is the mean-square end-to-end distance (of the unperturbed chain without excluded volume). Thus, we may compare the values of A_K instead of $(\langle S^2\rangle/x_w)_{x_w=\infty}$, since the two polymers have approximately the same values of M_L and also M_0. From eqs 7, 13, and 17, we have

$$A_K = c_\infty\lambda^{-1} \tag{18}$$

where $c_\infty \le 1$, as seen from eq 14, so that $A_K \le \lambda^{-1}$, the equality holding only for the KP chain ($\kappa_0 = 0$). Thus, A_K is in general not correlated to the chain stiffness, although λ^{-1} is its measure from the theoretical standpoint.

In Table VI are given the values of c_∞ and A_K (along with λ^{-1}) calculated from eqs 14 and 17 (or eq 18) with the model parameters given in Table V for a-PMMA and a-PS.[36] As seen from Table VI, despite the fact that A_K is smaller for a-PMMA than for a-PS, which comes from c_∞, λ^{-1} is larger for the former than for the latter. In the next subsection, the discussion is expanded, giving a picture of chain conformations for the two polymers.

Local Conformation of the a-PMMA Chain. For convenience, we begin by discussing the characteristic helix of the HW model, whose radius ρ and pitch h are given

Table V
Values of the HW Model Parameters

polymer (f_r)	solvent	temp, °C	$\lambda^{-1}\kappa_0$	$\lambda^{-1}\tau_0$	λ^{-1}, Å	M_L, Å^{-1}	obsd quantity
a-PMMA (0.79)	acetonitrile	44.0	4.0	1.1	57.9	36.3	$\langle S^2\rangle$
a-PS (0.59)	cyclohexane	34.5	3.0	6.0	22.5	36.7	$\langle\Gamma^2\rangle$, $\langle S^2\rangle$

Table VI
Values of λ^{-1}, c_∞, and A_K

polymer (f_r)	λ^{-1}, Å	c_∞	A_K, Å
a-PMMA (0.79)	57.9	0.246	14.2
a-PS (0.59)	22.5	0.816	18.4

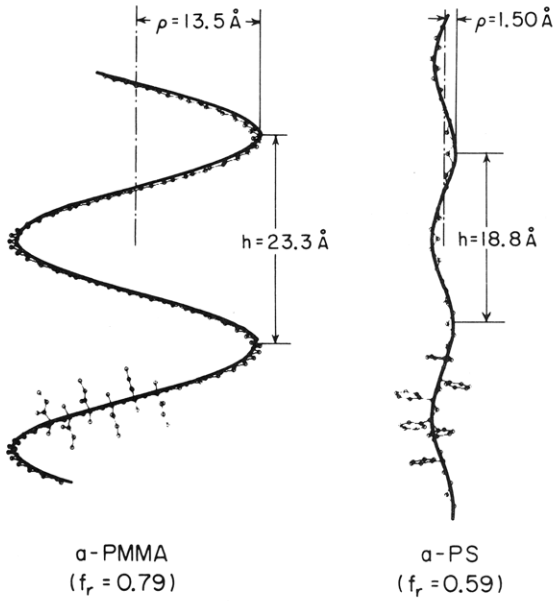

Figure 7. Schematic drawing of the conformations of the a-PMMA chain with $f_r = 0.79$ and the a-PS chain with $f_r = 0.59$ at the minimum of the potential energy. The heavy solid line indicates the HW chain contour (characteristic helix) for each polymer.

by $\rho = \kappa_0/(\kappa_0^2 + \tau_0^2)$ and $h = 2\pi\tau_0/(\kappa_0^2 + \tau_0^2)$. For the a-PMMA, we have $\rho = 13.5$ Å and $h = 23.3$ Å, if we use the values of κ_0 and τ_0 from Table V. In Figure 7 is schematically depicted this characteristic helix (thick curve) along with the corresponding conformation that the chain takes at the minimum of potential energy. For comparison, those for the a-PS are also shown in the figure. We note that the values of ρ and h for the latter have been calculated by the use of the parameters in Table V and therefore are somewhat different from those previously determined from $[\eta]$.[3] There is a remarkable difference between the two helices in shape; ρ for a-PMMA is much larger than that for a-PS, while they have almost the same h. The large ρ for the former arises from a predominance of the tt conformation for its racemic diads along with an appreciable difference between the two successive bond angles in its main chain.[7,19]

The actual conformation of the polymer chain in dilute solution is, of course, different from such a regular structure, which is, to some extent, destroyed because of thermal fluctuations. The extent may be measured by the parameter λ^{-1}; the larger λ^{-1} is, the larger the preservation of the regular helix. In order to illustrate the situation, we have generated HW Monte Carlo chains corresponding to a-PMMA and a-PS, both of contour length $L = 1000$ Å. Note that this value of L corresponds to x_w such that their $\langle S^2\rangle/x_w$ values reach nearly the respective asymptotic values. The details of the Monte Carlo method are given in Appendix B. In Figure 8 are depicted projections of representative instantaneous chain contours of the two

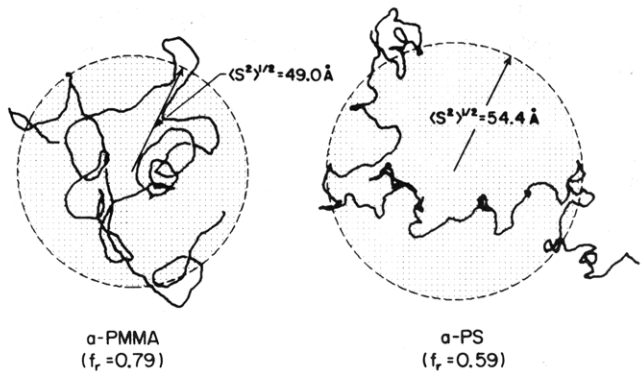

Figure 8. Projections of representative instantaneous contours of HW Monte Carlo chains corresponding to the a-PMMA and the a-PS of contour length $L = 1000$ Å such that their radii of gyration, S, are just equal to their respective $\langle S^2\rangle^{1/2}$. The shaded circular domain indicates the projection of the sphere whose radius is equal to $\langle S^2\rangle^{1/2}$ for each model chain.

polymers such that their radii of gyration, S, are just equal to the respective values of $\langle S^2\rangle^{1/2}$.

From Figure 8, it is clearly seen that the chain contour of the a-PMMA is rather smooth with retention of large helical portions, the one observed, for instance, at the right bottom of the picture being close to one turn of the characteristic helix in size. In contrast to this, the contour of the a-PS turns and twists more randomly and on the much smaller length scales. These result from the differences between the two chains in the characteristic helix and the value of λ^{-1}. The smaller C_∞ and A_K or $(\langle S^2\rangle/x)_{x=\infty}$ for the a-PMMA are due to the retention of large helical portions.

Concluding Remarks

We have been able to determine rather unambiguously the HW model parameters for a-PMMA from an analysis of the experimental data only for $\langle S^2\rangle$. A similar analysis may be possible for $[\eta]$ and $\langle\Gamma^2\rangle$ for the same a-PMMA samples, and this will be done in subsequent papers. It is then interesting to examine whether all these along with other dilute solution properties may well be explained consistently with the same model parameters. For PMMA, it is also important to investigate possible effects of the tacticity on or the f_r dependence of these properties.

Appendix A. The RIS Model Parameters

In the a-PMMA chain under consideration, the terminal α carbon, C^α, having two methyl (Me) groups is optically inactive, while the other having one Me group is optically active (or asymmetric). For convenience, we number the skeletal bonds in the chain with the degree of polymerization, x, from the former end, regarding one of the Me→C^α bonds as the first bond and the C^α→Me bond at the latter end as the $2x$th bond, and then treat the former C^α as the "asymmetric" carbon formally. The $2x + 1$ skeletal carbon atoms are thus numbered 0, 1, ..., $2x + 1$ from the former end. In this appendix, we give the elements of the statistical weight matrices $\mathbf{U}_2$, $\mathbf{U}_3$, and $\mathbf{U}_{2x-1}$ for the pairs of bonds (1, 2), (2, 3), and $(2x - 2, 2x - 1)$ for the three RIS models mentioned in the text. For the weight matrix $\mathbf{U}_j$ ($j = 4, 5, ..., 2x - 2$) for the pair of bonds $(j - 1, j)$ of each model, we may use the one given in the

original papers,[22-24] as noted in the text. For all the three models, we treat the first diad as "meso", for convenience. As before,[2] we adopt the new Flory convention[37] to describe the stereochemical configuration of the asymmetric chain.

We first consider $\mathbf{U}_2$ and $\mathbf{U}_3$. Although the $\bar{g}$ conformation is inhibited for the internal bonds in the 2-state model, it must be restored for the second bond since the first-order interaction for $\bar{g}$ is equivalent to that for the t conformation. Thus, we permit this bond to take three rotational isomeric states t, g, and $\bar{g}$ (−120°) and denote their statistical weights of the first-order interaction by η, $1/\rho$, and η, respectively. Note that the first bond is fixed as t in this model. Following Flory et al.,[37] $\mathbf{U}_2$ and $\mathbf{U}_3$ for the 2-state model may then be written in the form

$$\mathbf{U}_2 = \begin{pmatrix} 1 & 1 & 1 \\ 0 & 0 & 0 \end{pmatrix} \quad \text{(2-state RIS)} \qquad \text{(A1)}$$

$$\mathbf{U}_3 = \begin{pmatrix} 1 & \alpha & \\ \alpha/\rho & \alpha^2/\beta\rho & \\ \beta & \alpha & \end{pmatrix} \quad \text{(2-state RIS)} \qquad \text{(A2)}$$

where α and β are the parameters defined by eqs 11 and 12 of ref 37. They are written in terms of η combined with the statistical weights for the second-order interaction. The values of α and β have been obtained to be 0.279 and 3.63 at 44.0 °C, respectively, from the relations $\alpha = 1.6 \exp(-1100/RT)$ and $\beta = 1.4 \exp(600/RT)$ given in ref 22 with R the gas constant. The statistical weight ρ may be considered to be equivalent to the one defined for the 3-state model and given by the third of eq 6 of ref 24. It has been evaluated to be 0.104 at 44.0 °C, from the equation, $\rho = 0.87 \exp(-1340/RT)$, obtained from the corresponding equation of ref 24 by replacing the value 1016 for the energy E_ρ by 1340 (see below).

In the 6-state model, we assume that the second bond may take the six states as well as the internal bonds and that the first-order interactions for the $\bar{g}_+$, $\bar{g}_-$, and g_+ conformations for the second bond are equivalent to those for the t_-, t_+, and g_- conformations, respectively. We also assume that the first bond takes only t_+ and t_-, so that we have $\mathbf{U}_1 = (1\,1\,0\,0\,0\,0)$. Following Vacatello and Flory,[23] $\mathbf{U}_2$ and $\mathbf{U}_3$ may then be written in the form

$$\mathbf{U}_2 = \begin{pmatrix} u_{t_-t_-} & 1 & u_{t_-g_-} & u_{t_-g_-} & 1 & u_{t_-t_-} \\ 1 & u_{t_+t_+} & u_{t_+g_-} & u_{t_+g_-} & u_{t_+t_+} & 1 \\ 0 & 0 & 0 & 0 & 0 & 0 \\ 0 & 0 & 0 & 0 & 0 & 0 \\ 0 & 0 & 0 & 0 & 0 & 0 \\ 0 & 0 & 0 & 0 & 0 & 0 \end{pmatrix} \quad \text{(6-state RIS)} \qquad \text{(A3)}$$

$$\mathbf{U}_3 = \begin{pmatrix} 0 & 1 & 0 & \alpha'\beta' & 0 & \alpha'\bar{\alpha} \\ 1 & 0 & \alpha'\beta' & 0 & \alpha'\bar{\alpha} & 0 \\ 0 & \alpha'\beta' & 0 & \beta'^2 & 0 & \bar{\alpha}\beta' \\ \alpha'\beta' & 0 & \beta'^2 & 0 & \bar{\alpha}\beta' & 0 \\ 0 & \alpha'^2 & 0 & \alpha'\beta' & 0 & \bar{\rho} \\ \alpha'^2 & 0 & \alpha'\beta' & 0 & \bar{\rho} & 0 \end{pmatrix} \quad \text{(6-state RIS)} \qquad \text{(A4)}$$

where $u_{t_-t_-}$, $u_{t_-g_-}$, $u_{t_+t_+}$, and $u_{t_+g_-}$ in $\mathbf{U}_2$ are the parameters defined by eq 7 of ref 23, and α', $\bar{\alpha}$, β', and $\bar{\rho}$ in $\mathbf{U}_3$ are identical with α, $\bar{\alpha}$, β, and $\bar{\rho}$ given in ref 23, respectively. The parameters in $\mathbf{U}_2$ have been evaluated, from eq 8 with the energy parameters listed in Table VI of ref 23, to be 1.56×10^{-1}, 3.98×10^{-4}, 4.00, and 1.05×10^{-3} at 44.0 °C, respectively. The values of the parameters in $\mathbf{U}_3$ have also been obtained, from eq 8 of ref 23, to be 2.27, 3.26, 265, and 19.3 at 44.0 °C, respectively. Although the values of $u_{t_-g_-}$ and $u_{t_+g_-}$ in $\mathbf{U}_2$ are not certain, we simply assume that they are the same as those for the internal bond pairs, since the values of $\langle S^2 \rangle$ have been found to be insensitive to change in their values.

In the 3-state model, the first-order interaction for $\bar{g}$ for the second bond is equivalent to that for t, as in the 2-state model. Thus, we denote the statistical weights for the first-order interaction for t, g, and $\bar{g}$ for the second bond by η, $1/\rho$, and η, respectively. Note that the first bond is fixed as t in this model. Following Sundararajan,[24] $\mathbf{U}_2$ and $\mathbf{U}_3$ may then be written in the form

$$\mathbf{U}_2 = \begin{pmatrix} 1 & 1 & 1 \\ 0 & 0 & 0 \\ 0 & 0 & 0 \end{pmatrix} \quad \text{(3-state RIS)} \qquad \text{(A5)}$$

$$\mathbf{U}_3 = \begin{pmatrix} 1 & \alpha & \beta\rho \\ \alpha/\rho & \alpha^2/\beta\rho & \alpha \\ \beta & \alpha & \rho \end{pmatrix} \quad \text{(3-state RIS)} \qquad \text{(A6)}$$

where α and β have been evaluated to be 0.174 and 3.77 at 44.0 °C, respectively, from eq 12 of ref 24, by changing the value of the energy E_α from 991 to 1000 and that of E_β from −358 to −1000. The value of ρ is the same as given above for the 2-state model. These values of α, β, and ρ have been determined so that the calculated asymptotic value of $\langle S^2 \rangle / x$ agrees with the observed one. We have also used them for the internal bonds.

Next, we consider $\mathbf{U}_{2x-1}$ for the pair of bonds $(2x-2, 2x-1)$, regarding the $(2x-1)$th bond as a portion of a poly(methyl acrylate) (PMA) chain. Thus, for the statistical weights for the first-order and second-order interactions, we use those given for PMA by Ojalvo et al.,[38] where for the $(2x-1)$th bond, $\bar{g}$ is inhibited and only the two rotational states t(10°) and g(110°) are permitted. For the $(2x-2)$th bond, we denote the statistical weights for the first-order interaction for t and g by $\tilde{\eta}$ and 1, respectively, in the 2-state and 3-state models and then assume that the weight for $\bar{g}$ may be equated to $\tilde{\eta}\rho$ in the 3-state model. $\mathbf{U}_{2x-1}$ for meso and racemic diads may then be written for the three RIS models, as

$$\mathbf{U}_{2x-1} = \begin{pmatrix} \tilde{\eta}^2\omega'' & \tilde{\eta}\omega \\ \tilde{\eta}\omega' & \omega \end{pmatrix} \quad \text{for meso diad}$$

$$= \begin{pmatrix} \tilde{\eta}^2\omega' & \tilde{\eta}\omega' \\ \tilde{\eta}\omega' & \omega \end{pmatrix}$$

for racemic diad (2-state RIS) (A7)

$$\mathbf{U}_{2x-1}^{\mathrm{T}} = \begin{pmatrix} \tilde{\eta}\omega'' & \tilde{\eta}\omega'' & \tilde{\eta}\omega' & \tilde{\eta}\omega' & \tilde{\eta}\omega' & \tilde{\eta}\omega' \\ \omega & \omega & \omega & \omega & \omega' & \omega' \end{pmatrix} \quad \text{for meso diad}$$

$$= \begin{pmatrix} \tilde{\eta}\omega' & \tilde{\eta}\omega' & \tilde{\eta}\omega' & \tilde{\eta}\omega' & \tilde{\eta}\omega'' & \tilde{\eta}\omega'' \\ \omega' & \omega' & \omega & \omega & \omega & \omega \end{pmatrix}$$

for racemic diad (6-state RIS) (A8)

$$\mathbf{U}_{2x-1} = \begin{pmatrix} \tilde{\eta}^2\omega'' & \tilde{\eta}\omega \\ \tilde{\eta}\omega' & \omega \\ \tilde{\eta}^2\rho\omega' & \tilde{\eta}\rho\omega' \end{pmatrix} \quad \text{for meso diad}$$

$$= \begin{pmatrix} \tilde{\eta}^2\omega' & \tilde{\eta}\omega' \\ \tilde{\eta}\omega' & \omega \\ \tilde{\eta}^2\rho\omega'' & \tilde{\eta}\rho\omega \end{pmatrix}$$

for racemic diad (3-state RIS) (A9)

where the superscript T indicates the transpose, $\tilde{\eta}$, ω, and

ω' are identical with η, ω, and ω' given in ref 38, respectively, and ω'' is assumed to be given by $\omega'' = (\omega_i'' + \omega_d'')/2$ with ω_i'' and ω_d'' defined in ref 38. The values of $\tilde{\eta}$, ω, ω', ω_i'', and ω_d'' have been obtained to be 1.56, 2.93×10^{-3}, 3.19×10^{-2}, 8.4×10^{-2}, and 1.92×10^{-1} at 44.0 °C, respectively, by the use of the energy parameters listed in Tables IV and VI of ref 38. Recall that $\mathbf{U}_{2x}^{\mathrm{T}} = (1, 1)$ in any case.

Appendix B. HW Monte Carlo Chains

In order to generate instantaneous configurations of the contour of the HW chain (in a thermal bath), we consider its discrete analogue as in the case of its dynamics.[6] We divide the HW chain of contour length L into N identical parts of contour length Δs; i.e., $L = N\Delta s$. For the case of $\lambda\Delta s \ll 1$, the bond vector $\mathbf{a}_p$ ($p = 1, 2, ..., N$) as defined as the vector distance between the contour points $(p-1)\Delta s$ and $p\Delta s$ may be assumed to be of length Δs and in the direction of the vector tangential to the contour or the ζ axis of a localized Cartesian coordinate system (ξ, η, ζ) affixed at the contour point $(p-1)\Delta s$. Let $\Delta\Omega_p$ ($p = 1, 2, ..., N-1$) be the infinitesimal rotation vector by which the localized coordinate system at the contour point $p\Delta s$ is obtained from the one at the contour point $(p-1)\Delta s$, let $\Delta\Omega_{p\xi}$, $\Delta\Omega_{p\eta}$, and $\Delta\Omega_{p\zeta}$ be the Cartesian components of $\Delta\Omega_p$ expressed in the latter system, and let $\Delta\Omega_p = (|\Delta\Omega_p|, \theta_p, \varphi_p)$ in spherical polar coordinates of that system.

The transformation from the latter to the former system may then be represented by the transformation matrix $\mathbf{T}_p$ defined by

$$\mathbf{T}_p = \mathbf{A}^{-1}(\theta_p, \varphi_p)\cdot\mathbf{R}(|\Delta\Omega_p|)\cdot\mathbf{A}(\theta_p, \varphi_p) \tag{B1}$$

where the rotation matrices $\mathbf{A}(\theta, \varphi)$ and $\mathbf{R}(\psi)$ are given by

$$\mathbf{A}(\theta, \varphi) = \begin{pmatrix} \cos\theta\cos\varphi & \cos\theta\sin\varphi & -\sin\theta \\ -\sin\varphi & \cos\varphi & 0 \\ \sin\theta\cos\varphi & \sin\theta\sin\varphi & \cos\theta \end{pmatrix} \tag{B2}$$

$$\mathbf{R}(\psi) = \begin{pmatrix} \cos\psi & \sin\psi & 0 \\ -\sin\psi & \cos\psi & 0 \\ 0 & 0 & 1 \end{pmatrix} \tag{B3}$$

By the use of the transformation matrices $\mathbf{T}_p$ thus defined, the pth bond vector $\mathbf{a}_p$ ($p = 2, 3, ..., N$) expressed in the localized system at the countour point 0 may be written as

$$\mathbf{a}_p = \mathbf{T}_1^{-1}\cdot\mathbf{T}_2^{-1}\cdot\cdots\cdot\mathbf{T}_{p-1}^{-1}\cdot\mathbf{a} \tag{B4}$$

where $\mathbf{a}$ is the pth bond vector $\mathbf{a}_p$ in the $(p-1)$th system, so that $\mathbf{a}$ is $\mathbf{a}_1 = (0, 0, \Delta s)$ in the 0th system.

An instantaneous configuration of this entire HW chain may be generated by jointing the bond vectors $\mathbf{a}_p$ successively, so that we have only to generate a set of the $N-1$ infinitesimal rotation vectors $\Delta\Omega_p$ ($p = 1, 2, ..., N-1$). The elastic potential (bending and torsional) energy of the HW chain per unit contour length is written in terms of the "angular velocity" vector of the localized coordinate system, which is given by eq 1 of ref 6 or eq 14 of ref 39 with $\alpha = \beta = k_B T/2\lambda$. Assuming that the angular velocity takes the constant value $\Delta\Omega_p/\Delta s$ between the contour points $(p-1)\Delta s$ and $p\Delta s$ for $\lambda\Delta s \ll 1$, we write the potential energy U_p associated with the rotation $\Delta\Omega_p$ in the form

$$U_p = \frac{1}{4\lambda\Delta s}[(\Delta\Omega_{p\xi})^2 + (\Delta\Omega_{p\eta} - \kappa_0\Delta s)^2 + (\Delta\Omega_{p\zeta} - \tau_0\Delta s)^2] \tag{B5}$$

in units of $k_B T$. We can then readily generate $\Delta\Omega_p$ by the introduction of the Boltzmann factor e^{-U_p} as the equilibrium probability distribution function of $\Delta\Omega_p$.

For the generation of the chain, $\lambda\Delta s$ must be taken to be as small as possible. We have taken $\lambda\Delta s = 0.02$ for the calculation in the text.

References and Notes

(1) Konishi, T.; Yoshizaki, T.; Yamakawa, H. *Polym. J.* **1988**, *20*, 175.
(2) Konishi, T.; Yoshizaki, T.; Shimada, J.; Yamakawa, H. *Macromolecules* **1989**, *22*, 1921.
(3) Einaga, Y.; Koyama, H.; Konishi, T.; Yamakawa, H. *Macromolecules* **1989**, *22*, 3419.
(4) Konishi, T.; Yoshizaki, T.; Saito, T.; Einaga, Y.; Yamakawa, H. *Macromolecules* **1990**, *23*, 290.
(5) Yamakawa, H. *Annu. Rev. Phys. Chem.* **1984**, *35*, 23.
(6) Yamakawa, H. In *Molecular Conformation and Dynamics of Macromolecules in Condensed Systems*; Nagasawa, M., Ed.; Elsevier: Amsterdam, 1988; p 21.
(7) Yamakawa, H.; Fujii, M. *J. Chem. Phys.* **1976**, *64*, 5222.
(8) Yamakawa, H.; Fujii, M.; Shimada, J. *J. Chem. Phys.* **1979**, *71*, 1611.
(9) Yoshizaki, T.; Nitta, I.; Yamakawa, H. *Macromolecules* **1988**, *21*, 165.
(10) Konishi, T.; Tamai, Y.; Fujii, M.; Einaga, Y.; Yamakawa, H. *Polym. J.* **1989**, *21*, 329.
(11) Schulz, G. V.; Kirste, R. G. *Z. Phys. Chem.* **1961**, *30*, 171.
(12) Fox, T. G; Kinsinger, J. B.; Mason, H. F.; Schuele, E. M. *Polymer* **1962**, *3*, 71.
(13) Fox, T. G *Polymer* **1962**, *3*, 111.
(14) Kirste, R. G.; Wunderlich, W. *Makromol. Chem.* **1964**, *73*, 240.
(15) Wunderlich, W.; Kirste, R. G. *Ber. Bunsen-Ges. Phys. Chem.* **1964**, *68*, 646.
(16) Patrone, E.; Bianchi, U. *Makromol. Chem.* **1966**, *94*, 52.
(17) Kirste, R. G.; Wunderlich, W. *Z. Phys. Chem.* **1968**, *58*, 133.
(18) Kirste, R. G.; Kruse, W. A.; Ibel, K. *Polymer* **1975**, *16*, 120.
(19) Yoon, D. Y.; Flory, P. J. *Polymer* **1975**, *16*, 645.
(20) Kratky, O.; Porod, G. *Recl. Trav. Chim.* **1949**, *68*, 1106.
(21) Yamakawa, H.; Shimada, J. *J. Chem. Phys.* **1985**, *83*, 2607.
(22) Sundararajan, P. R.; Flory, P. J. *J. Am. Chem. Soc.* **1974**, *96*, 5025.
(23) Vacatello, M.; Flory, P. J. *Macromolecules* **1986**, *19*, 405.
(24) Sundararajan, P. R. *Macromolecules* **1986**, *19*, 415.
(25) Webster, O. W.; Hertler, W. R.; Sogah, D. Y.; Farnham, W. B.; RajanBabu, T. V. *J. Am. Chem. Soc.* **1983**, *105*, 5706.
(26) Müller, M. A.; Stickler, M. *Makromol. Chem., Rapid Commun.* **1986**, *7*, 575.
(27) (a) Rubingh, D. N.; Yu, H. *Macromolecules* **1976**, *9*, 681. (b) Berry, G. C. *J. Chem. Phys.* **1966**, *44*, 4550.
(28) Spěváček, J.; Schneider, B. *Makromol. Chem.* **1975**, *176*, 3409.
(29) Chûjô, R.; Hatada, K.; Kitamaru, R.; Kitayama, T.; Sato, H.; Tanaka, Y. *Polym. J.* **1987**, *19*, 413.
(30) Huber, K.; Stockmayer, W. H. *Macromolecules* **1987**, *20*, 1400.
(31) Yamakawa, H. *Macromolecules* **1977**, *10*, 692.
(32) Flory, P. J. *Statistical Mechanics of Chain Molecules*; Interscience: New York, 1969.
(33) Flory, P. J. *Macromolecules* **1974**, *7*, 381.
(34) Miyaki, Y. Ph.D. Thesis, Osaka University, 1981.
(35) Miyaki, Y.; Einaga, Y.; Fujita, H.; Fukuda, M. *Macromolecules* **1980**, *13*, 588.
(36) Although in ref 3, the value of A_K for a-PS was calculated from eq 18 with eq 14 of this paper, the description of it therein is wrong.
(37) Flory, P. J.; Sundararajan, P. R.; DeBolt, L. C. *J. Am. Chem. Soc.* **1974**, *96*, 5015.
(38) Ojalvo, E. A.; Saiz, E.; Masegosa, R. M.; Hernández-Fuentes, I. *Macromolecules* **1979**, *12*, 865.
(39) Yamakawa, H.; Shimada, J. *J. Chem. Phys.* **1978**, *68*, 2140.

Registry No. PMMA, 9011-14-7.